Aldolase Exists in Both the Fluid and Solid Phases of Cytoplasm

Len Pagliaro and D. Lansing Taylor

Department of Biological Sciences, Center for Fluorescence Research in Biomedical Sciences, Carnegie-Mellon University, Pittsburgh, Pennsylvania 15213

Abstract. We have prepared a functional fluorescent analogue of the glycolytic enzyme aldolase (rhodamine [Rh]-aldolase), using the succinimidyl ester of carboxytetramethyl-rhodamine. Fluorescence redistribution after photobleaching measurements of the diffusion coefficient of Rh-aldolase in aqueous solutions gave a value of 4.7×10^{-7} cm²/s, and no immobile fraction. In the presence of filamentous actin, there was a 4.5-fold reduction in diffusion coefficient, as well as a 36% immobile fraction, demonstrating binding of Rh-aldolase to actin. However, in the presence of a 100-fold molar excess of its substrate, fructose 1,6-diphosphate, both the mobile fraction and diffusion coefficient of Rh-aldolase returned to control levels, indicating competition between substrate binding and actin cross-linking. When Rh-aldolase was microinjected into Swiss 3T3 cells, a relatively uniform intracellular distribution of fluorescence was observed. However, there were significant spatial differences in the in vivo diffusion coefficient and mobile fraction of Rh-aldolase measured with fluorescence redistribution after photobleaching. In the perinuclear region, we measured an apparent cytoplasmic diffusion coefficient of 1.1×10^{-7} cm²/s with a 23% immobile fraction; while measurements in the cell periphery gave a value of 5.7×10^{-8} cm²/s, with no immobile fraction. Ratio imaging of Rh-aldolase and FITC-dextran indicated that FITC-dextran was relatively excluded from stress fiber domains. We interpret these data as evidence for the partitioning of aldolase between a soluble fraction in the fluid phase and a fraction associated with the solid phase of cytoplasm. The partitioning of aldolase and other glycolytic enzymes between the fluid and solid phases of cytoplasm could play a fundamental role in the control of glycolysis, the organization of cytoplasm, and cell motility. The concepts and experimental approaches described in this study can be applied to other cellular biochemical processes.

ALTHOUGH glycolytic metabolism is well-defined at the biochemical level, the dynamic and spatial organization of glycolysis in living cells has not been characterized to date. After the elucidation of mitochondrial structure and function 35 years ago (28) it was generally assumed that a corresponding organelle for glycolysis must exist. Efforts to isolate and to characterize such an organelle were unsuccessful, leading de Duve (26) to conclude that the long-sought "glycolytic particle" did not exist. As a result, the current concept of in vivo glycolytic metabolism is based on an assumption of dilute solution chemistry, due largely to the absence of evidence for a discrete glycolytic organelle.

There has been evidence for over 20 years that some glycolytic enzymes bind to structural proteins, particularly actin. The interaction of aldolase with actin has been demonstrated histochemically (8, 61), biochemically (5, 6, 8, 69), ultrastructurally (16, 52), and with immunofluorescence techniques (27). In fact, aldolase was among the first actin-binding proteins to be identified (10), although this interaction was not considered specific at the time. It has since been well-characterized in terms of both its native structure, enzymatic activity, and its actin-binding qualities. Some of the characteristics of vertebrate striated muscle aldolase are reviewed in Table I. Aldolases from other mammalian sources are reasonably well-conserved (56).

The potential significance of the localization of glycolytic enzymes has been indicated by reconstitution experiments under conditions of physiological ionic strength and protein concentration (15), and in the presence of the regulatory proteins of skeletal muscle (75). This work suggested that previously reported "glycolytic component" complexes (13, 14, 34) were actually complexes of glycolytic enzymes with structural proteins, and implied that the glycolytic particle might exist as such a complex. The model for the cytoplasmic organization of glycolytic enzymes that has emerged from Clarke and Masters' work is that there is a "plating" of glycolytic enzymes around the filamentous actin (F-actin)[1] core of microfilaments (48). Masters proposed a dynamic

1. *Abbreviations used in this paper*: D_{aq}, aqueous diffusion coefficient; D_{cyto}, apparent cytoplasmic diffusion coefficient; D/P, dye/protein ratio; F-actin, filamentous actin; FDP, fructose 1,6-diphosphate; FRAP, fluorescence redistribution after photobleaching; Rh, rhodamine.

Table I. Properties of Vertebrate Striated Muscle Aldolase

Property		Reference No.
Molecular mass	160,000 D	39
Conformation	heterotetramer	33
	361 residues per monomer	33
Subunits	2× α (asn at 358)*	39
	2× β (asp at 358)	39
Substrate	FDP	
Cellular concentrations	aldolase 88 μM	calculated from 65
	FDP 160 μM	calculated from 67

* Subunits are identical except for this single-residue difference.

three-way equilibrium among monomeric actin, F-actin, and glycolytic enzymes, resulting in a microdomain of glycolytic enzymes surrounding actin filaments. If this model is correct, then glycolytic enzymes could exist as a solid state chemical reaction series and the prevailing view that glycolytic enzymes are dissolved in the aqueous phase of the cytoplasm is only partially correct. Alternatively, enzymes associated with the solid phase of cytoplasm could be a kinetically modified subset of glycolytic enzymes (50).

It has also been suggested that glycolytic enzymes have a functional duality, playing structural roles, as well as their established catalytic roles (18). In such a dual role, glycolytic enzymes could be integrators of cytoplasmic structure and function, by binding to actin as well as to substrate. This exciting idea is supported by evidence obtained in vitro that (*a*) the actin-gelling activity of aldolase is inhibited by its substrate fructose 1,6-diphosphate (FDP; 18), (*b*) the kinetics of aldolase activity are modified by the actin-containing filaments of skeletal muscle (74), and (*c*) the actin filaments of muscle tissue perturbed by electrical stimulation (19) or anoxia (20) bind a substantially higher percentage of aldolase than do those of unperturbed muscle. In view of the above evidence, we agree with Clarke et al. (21) that aldolase–actin interactions cannot be prejudged as "non-specific" (24).

Investigations of glycolysis by biochemical methods in vitro, as well as histochemical and ultrastructural approaches in fixed cells, have been valuable; however these approaches have serious limitations: cells cannot be modeled as dilute solutions, temporal variations cannot be detected, and spatial information is lost (23, 31, 46, 47, 77). Our approach to studying the possible relationship of glycolysis to cytoplasmic structure was to develop a fluorescent analogue of aldolase (rhodamine [Rh]-aldolase) and to perform experiments on individual living Swiss 3T3 cells using fluorescent analogue cytochemistry, fluorescence redistribution after photobleaching (FRAP), and digital imaging (71, 72). We found a relatively uniform distribution of Rh-aldolase in cells, but significant spatial differences in both its diffusion coefficient[2] and mobile fraction. The evidence we present is consistent with the concept that glycolytic enzymes can exist in both the fluid phase and solid phase of cytoplasm.

2. The term diffusion coefficient can only be used rigorously for measurements made in aqueous solution (D_{aq}). We refer to cytoplasmic mobility as an apparent diffusion coefficient (D_{cyto}) to compare aqueous and cytoplasmic values.

Materials and Methods

Materials

All biochemicals were purchased from Sigma Chemical Co. (St. Louis, MO) unless otherwise specified.

Fluorescent Labeling of Aldolase

Purified rabbit muscle aldolase was reacted with carboxytetramethylrhodamine succinimide ester (Molecular Probes Inc., Eugene, OR) by a method analogous to that used in the iodination of aldolase with an *N*-hydroxysuccinimide acylating agent (11, 20). A 3.0 M ammonium sulfate suspension containing 5 mg of aldolase in 230 μl was dialyzed to equilibrium against 1,000 vol of 3 mM Tris-HCl and 10 mM EDTA at pH 7.5 (labeling buffer). The dye was dissolved in dimethyl formamide (Eastman Kodak Co., Rochester, NY) shortly before use. Immediately before reaction, a 10-fold molar excess of dye/dimethyl formamide solution (based on the tetrameric weight of aldolase) was dissolved in a volume of 200 mM borate buffer, pH 8.5, equal to that of the dialyzed aldolase solution. This mixture was then added dropwise with continual stirring to the aldolase, and incubated on ice for 15 min. The reaction was terminated by adding sufficient 1.0 M ethanolamine to bring the final concentration to 100 mM, and was then stirred on ice for an additional 3 min. The reacted mixture was dialyzed in collodion bags (Schleicher and Schuell, Inc., Keene, NH) in the dark on ice for 48 h against four changes of labeling buffer to remove free dye. The final concentration of Rh-aldolase was 2–4 mg/ml, and it could be stored on ice for 1 wk with an enzymatic activity loss of ⩽1% per day. For assays of activity, parallel batches of aldolase were prepared in which a control was treated identically to the Rh-aldolase, except that no dye was present in the aliquot of dimethylformamide which was added to the reaction buffer (unlabeled controls).

Protein Assay

The protein assay used in these experiments was adapted from the Schacterle and Pollack (59) modification of the Lowry et al. (41) assay. All standards and samples were read at 750 nm (instead of 650 nm) to minimize interference from the fluorochrome absorbance maximum at 557 nm in the labeled species. The dye/protein ratio (D/P) of the labeled species was calculated by standard methods (62), using a molar extinction coefficient for the dye of 55,000 M^{-1} cm^{-1} (product data from Molecular Probes, Inc.).

Fluorescence Spectroscopy

Appropriately diluted samples of free dye or Rh-aldolase in the presence or absence of FDP were scanned using the photon counting mode of a spectrofluorometer system (model Fluorolog 2; Spex Industries, Inc., Edison, NJ). For excitation spectra, emission at 583 nm was monitored, and the excitation wavelength for emission spectra was 557 nm, using a slit bandwidth of ~1 nm in both cases. Rayleigh scatter peaks, at 583 and 557 for excitation and emission spectra, respectively, (3–4 points each), were removed manually after the scans.

Column Chromatography

A 10-mm × 45-cm Sephacryl S-300 (Pharmacia Fine Chemicals, Piscataway, NJ) column was equilibrated with a buffer consisting of 50 mM KCl, 1 mM EDTA, and 10 mM Tris-HCl, pH 7.5 (column buffer) at 4°C. Samples of aldolase and Rh-aldolase were dialyzed against several changes of column buffer, loaded on the column, and eluted at constant pressure using a peristaltic pump; 1.0 ml fractions were collected, and the absorbance of fractions was read at 280 nm.

FITC-Dextran

FITC-dextran of 156,500 mol wt was size fractionated over a 45-mm × 1-m S-300 column equilibrated with column buffer. The fractions constituting the central 60% of the Gaussian elution profile were pooled, dialyzed extensively against distilled water at 4°C, lyophilized, stored frozen, and resuspended into the desired buffer before use. Minor leading and trailing

elution peaks, as well as the tails of the Gaussian peak, were discarded. The fractionated FITC-dextran had an elution profile similar to that of Rh-aldolase (K_{av} = 0.240), and FRAP measurements of fractionated FITC-dextran gave a diffusion coefficient similar to that of Rh-aldolase ($D_{37,aq}$ = 4.8 × 10^{-7}), with significantly less scatter than in the data for $D_{37,aq}$ unfractionated FITC-dextran.

Gel Electrophoresis

Rh-aldolase samples were run on 12.5% SDS-PAGE gels in the presence of β-mercaptoethanol using the modifications discussed by Standart et al. (68) of gel systems described previously (4, 38). Samples of 10–50 μg of protein were loaded, and the gels were viewed under longwave UV irradiation before Coomassie Blue staining.

Enzymatic Activity Assay

The V_{max} and K_m of fructose 1,6-diphosphate (FDP) cleavage by aldolase were determined using a coupled assay (58, 80). The oxidation of NADH when α-glycerophosphate dehydrogenase catalyzes the conversion of dihydroxyacetone phosphate to α-glycerophosphate was measured by the decrease in absorbance at 340 nm. The reaction mixture consisted of 50 mM Tris-HCl, 1 mM $MgCl_2$, 5 mM EDTA, 2.5 mM FDP, 0.2 mM NADH, and 15 μl (35 U) of a stock solution of α-glycerophosphate dehydrogenase and triose phosphate isomerase, at pH 7.5 in a total volume of 1 ml maintained at 25°C by a circulating waterbath. The reaction was initiated by addition of 5.0 μg of aldolase (in 10 μl of labeling buffer) to the mixture in a cuvette. The decrease in NADH absorbance was monitored with a chart recorder, and slopes of absorbance plots were calculated to determine activities of aldolase samples.

Falling Ball Viscometry

Falling ball viscometry was used to measure the apparent viscosities of mixtures of aldolase and actin. The conditions used were essentially those of Clarke et al. (18), and the procedure was that of MacLean-Fletcher and Pollard (45, see also 62). Actin prepared by the method of Spudich and Watt (64) was used at a final concentration of 1.0 mg/ml throughout, and the assay buffer consisted of 40 mM KCl, 1 mM $MgCl_2$, 0.5 mM dithiothreitol (DTT), and 10 mM imidazole, at pH 6.8 (imidazole buffer). 300 μl of each sample were prepared and drawn into three 100-μl capillaries (Clay Adams, Parsipanny, NJ). The tubes were capped with plasticine, incubated for 30 min in a waterbath at 37°C, measured in triplicate and the times averaged. Straight lines were fit to inverse velocities with a microcomputer spreadsheet using slope and intercept values determined with standard glycerol solutions (29, 30). We have reproducibly calculated apparent viscosities as high as 2,000 centipoise with this method.

Irradiation of Samples

The 514-nm line of an argon ion laser (Spectra Physics, Inc., Mountain View, CA) was used to perform calibrated irradiation of aldolase and aldolase–actin mixtures in 100-μl capillary tubes. Tubes were irradiated for 100 s at 1 W laser output. The laser beam was expanded from an initial diameter of 3 to 13 mm with a microscope objective and a convex lens. The expanded beam was then focused with a 34-mm focal length cylindrical lens to illuminate a rectangular area measuring 2 × 13 mm, yielding a measured power of 300 mW at the target with an irradiance of ~1.2 W/cm^2 (63).

For assays of actin-binding activity, 1-cm sections of the capillary tubes were masked with black vinyl electrical tape, and these windows were held at the beam focus by placing the tube in an optical clamp. Samples were prepared for falling ball viscometry as above, but drawn into masked tubes. The concentration of aldolase was 1.5 μM (0.24 mg/ml); when actin was present it was at a concentration of 1.0 mg/ml. After incubation, a window on each tube was irradiated and then inverse velocities were measured in the standard way. Apparent viscosity was measured in both irradiated and nonirradiated 1-cm sections of each tube.

For assays of enzymatic activity, a 25 μl sample of 1.0 μM (0.16 mg/ml) aldolase was drawn into the center of a capillary tube and both ends were plugged with plasticine. The aldolase sample (24 mm in length) was irradiated with two doses that overlapped by 1 mm. Both irradiated samples and nonirradiated controls were drawn into capillary tubes identically. Immediately after irradiation, the samples were expelled from the tubes and assayed for enzymatic activity (see above).

FRAP and Calculations of Diffusion Coefficients

FRAP experiments were performed by the Gaussian spot method of Axelrod et al. (9) essentially as described previously (43, 44). The 514 nm (for rhodamine) and 488 nm (for fluorescein) lines of an ion argon laser (Spectra Physics, Inc.) were focused through a Universal microscope equipped with epifluorescence optics (Carl Zeiss, Inc., Thornwood, NY). The irradiance of the monitoring beam at the specimen plane was ~3.9 W/cm^2, which was an ~6,000-fold attenuation of the bleaching beam. Bleaching times ranged from 5 to 50 ms; 15–25% bleaching gave the most consistent data. Spot radii, measured as described previously (43, 44), were between 6 and 22 μm, and fluorescence recovery was monitored for 12–18 s, which represented 15–20 half-times of recovery. FRAP curves were analyzed by the method of Yguerabide et al. (81) or Van Zoelen et al. (73); the two methods agreed well when equally good curve fits were compared. Percent mobile fractions, defined as the percent recovery in the experimental timecourse, were calculated according to Axelrod et al. (9)[3]. Data acquisition and analysis was performed using a program written in Asyst (Macmillan Software Co., New York, NY) running on an IBM PC-AT equipped with an IBM Data Acquisition and Control board.

In vivo diffusion coefficients were measured with a 63× Plan-Neofluar oil immersion objective (NA = 1.25; Carl Zeiss, Inc.) at 37°C in a modified (12) Sykes-Moore chamber (Bellco Glass, Inc., Vineland, NJ) using a temperature-controlled stage (Rainin Instrument Co., Inc., Woburn, MA). Neutral density filters were used to attenuate both the monitoring and bleaching beams for in vivo FRAP. For in vitro measurements, a 6.3× Plan Achromat objective (NA = 0.16; Carl Zeiss, Inc.) focused the beam on samples drawn into 100 μm flat capillaries (Vitro Dynamics, Inc., Rockaway, NJ) sealed in Flo-Texx (Lerner Laboratories, New Haven, CT). The capillaries were placed on black-anodized machined aluminum flats, on a brass constant-temperature stage connected to a circulating waterbath and monitored with a small thermocouple (Cole-Parmer Instrument Co., Chicago, IL). Mixtures of 1.0 mg/ml F-actin and 1.0 μM Rh-aldolase were prepared in imidazole buffer similarly to those used for falling ball viscometry; FITC-dextran–actin mixtures were prepared similarly with the substitution of 2 μM FITC-dextran in the place of aldolase.

Temperature conversions for in vitro FRAP data were calculated using the Stokes-Einstein equation and published values for the viscosity of water (78) using a microcomputer spreadsheet program.

Cell Culture and Preparation

Swiss 3T3 fibroblasts (ATCC-CCL92; American Type Culture Collection, Rockville, MD) were cultured and prepared as described previously (25).

Microinjection and Imaging

Approximately 5–10% of a cell volume (72) of a stock solution containing 2 mg/ml Rh-aldolase and 2 mg/ml FITC-dextran was microinjected into 3T3 cells (3). Injected cells were allowed to recover for 30 min to 24 h, then placed in a chamber on a temperature-controlled stage and imaged with the system described by Bright et al. (12). Briefly, a 63× Plan-Neofluar oil immersion objective (1.25 NA) with narrow bandpass rhodamine and fluorescein epifluorescence filter sets on a Universal microscope (Carl Zeiss, Inc.) was used to image the fluorescence signal on a camera (model ISIT; Dage-MTI, Inc., Wabash, MI). Images of 128 averaged video frames were background subtracted and processed on an image processor (model VDP 1800; VICOM Systems, Inc., Junction City, CA), and photographed with HP-5 film (Ilford Limited, Cheshire, England) from the high resolution display monitor. Rhodamine and fluorescein excitation image pairs (for Rh-aldolase and FITC-dextran, respectively) were processed similarly.

Results

Characterization of Aldolase Labeling

SDS-PAGE of Rh-aldolase samples revealed a single band with a M_r of approximately 41,000 (data not shown). Neither the α and β subunits of aldolase nor labeled and unlabeled molecules were distinguishable on these one-dimen-

3. mobile fraction = $(F_\infty - F_\varphi)/(F_0 - F_\varphi) * 100$; immobile fraction = $[1 - (F_\infty - F_\varphi)/(F_0 - F_\varphi)] * 100$.

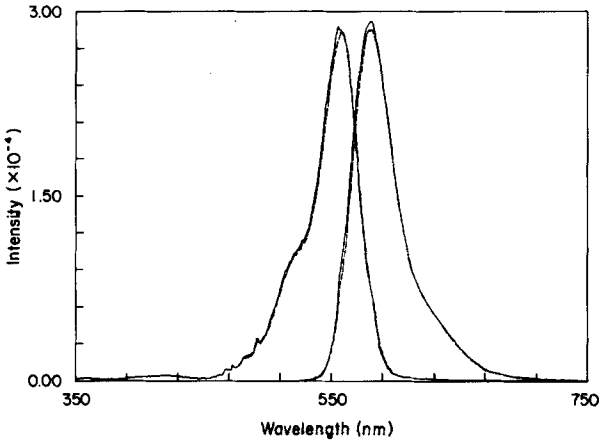

Figure 1. Excitation and emission spectra of Rh-aldolase. Spectra for Rh-aldolase (*dashed line*) and Rh-aldolase in the presence of a 100-fold molar excess of FDP (*solid line*).

sional gels. Extensive dialysis in colloidon bags proved as effective as G-100 exclusion chromatography at removing free carboxytetramethyl-rhodamine succinimide ester, and gave a better yield, although this is not the general rule with other fluorescent probes (62). After dialysis, very little free dye was visible at or ahead of the dye front of the gel under UV illumination, and the single 41,000-M_r band was both fluorescent, and Coomassie Blue stained.

The spectrophotometrically determined molar D/P of the Rh-aldolase tetramer was ~2.6:1.0. In the course of varying the molar excess of dye during labeling, we found that a distinct Poisson distribution of D/P existed. Different batches of Rh-aldolase were labeled with D/P of 1.2:1.0, 2.6:1.0, or 4.1:1.0 depending on the excess of dye available and the time of labeling. Batches labeled at 1.2:1.0 and 2.6:1.0 showed very similar activity; both lost ~10–15% of the enzymatic activity exhibited by the unlabeled molecule. Batches labeled at 4.1:1.0 showed a significant decrease (≈50%) in enzymatic activity. We chose the 2.6:1.0 D/P since that was the highest ratio attainable without substantial loss of activity.

The Rh-aldolase had absorption and emission maxima at 557 and 583 nm, respectively, yielding a Stokes shift of 26 nm (Fig. 1). Spectra taken in the presence of a 100-fold molar excess of FDP were nearly identical, showing no significant absorbance changes or spectral shifts upon substrate binding. These spectra very closely resemble that of the free dye when normalized for fluorescence intensity (data not shown).

Rh-Aldolase Is Biologically Active

Rh-aldolase eluted from an S-300 column with a profile similar to native aldolase (Fig. 2), demonstrating that the labeled molecule retained tetrameric conformation (49). The lead of the labeled species (K_{av} = 0.238 vs. K_{av} = 0.268) is probably due to a slight change in charge due to the fluorophore.

Rh-aldolase (D/P ~2.6:1.0) retained 85–90% of the enzymatic activity (V_{max}) of the native molecule. The K_m of Rh-aldolase was similar to that of the native molecule; both were 1.5–2.0 μM. These values are slightly higher than the published K_m value of 1.0 μM for aldolase (74), but internally consistent. Rh-aldolase had enzymatic activity only 1–2% lower than that of the unlabeled control (see Fig. 5, *Control*), demonstrating that the labeling conditions (pH shift, dimethyl formamide, ethanolamine) and not fluorophore binding directly, were primarily responsible for the 10–15% loss of activity in both groups.

We used falling ball viscometry to assay for actin-gelling activity of Rh-aldolase. Rh-aldolase was capable of producing actin gels of equal viscosity to those of the unlabeled control at slightly higher concentrations. Under our conditions, 1.25 μM aldolase reproducibly gelled 1.0 mg/ml actin to ≥1,500 centipoise, while 1.5 μM Rh-aldolase was required to reach that viscosity. Over the range of concentrations we studied, Rh-aldolase had an average of 81% of the actin-gelling activity of the unlabeled control (Fig. 3). This difference suggests that fluorophore binding affects actin-gelling activity slightly, and is consistent with our finding that the actin-gelling activity was more sensitive to higher D/P than the enzymatic activity. FDP inhibited gelation of R-aldolase–actin when added at time of mixing, and induced solation when added to gels.

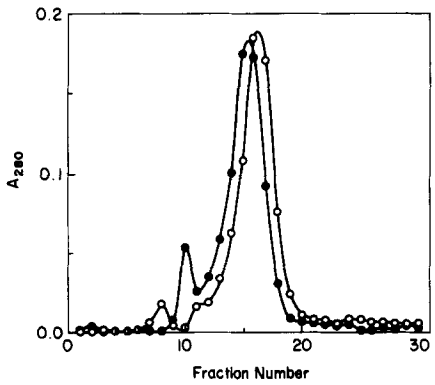

Figure 2. Elution profiles of aldolase and Rh-aldolase. Samples of aldolase (○) and Rh-aldolase (●) were eluted sequentially from the same S-300 column (see Materials and Methods); aldolase followed Rh-aldolase by ~10%; see text for discussion.

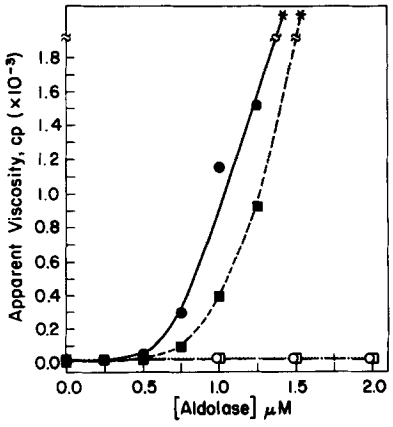

Figure 3. Low shear viscometry of Rh-aldolase–actin and aldolase–actin mixtures. The viscosity of 1.0 mg/ml F-actin in the presence of varying concentrations of unlabeled control aldolase (●), Rh-aldolase (■). Inhibition of actin gelation by 100 μM FDP is shown by controls for aldolase (○) and Rh-aldolase (□).

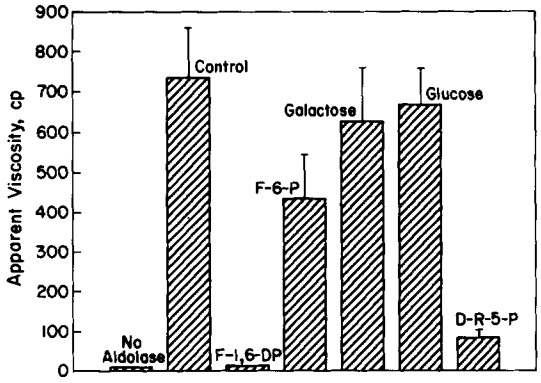

Figure 4. Specificity of actin-gelling activity of Rh-aldolase. The apparent viscosity of mixtures containing 1.0 mg/ml F-actin and 1 μM aldolase (except No. 1) is plotted; 100 M of substrate was used in each case.

We also used falling ball viscometry to investigate the degree of specificity of the aldolase–actin interaction. Measurements were made in the absence and presence of aldolase, and in the presence of 100 μM of each of the following sugars: FDP, fructose 6-phosphate, galactose, glucose, and D-ribose-5-phosphate (Fig. 4). While FDP reduced the viscosity of Rh-aldolase and actin gels 98.1% from the original level, fructose 6-phosphate gave only a 30.9% reduction. Clearly, there is a substantial degree of specificity in the substrate inhibition of aldolase–actin binding. Fructose 6-phosphate lowered the viscosity slightly more than either galactose or glucose, which had little effect, but allowed a viscosity of aldolase and actin 31-fold greater than FDP. D-ribose-5-phosphate inhibited gelation quite well, as predicted by its structural similarity to FDP.

FRAP Irradiation Does Not Destroy Rh-Aldolase Activity

Since Rh-aldolase is a fluorescent analogue of an enzyme it was important to know the degree to which the irradiation necessary in FRAP measurements reduced its activity. We used calibrated irradiation of samples of Rh-aldolase and Rh-aldolase–actin mixtures to determine the effect of irradiation on both enzymatic and actin-gelling activities. The irradiation dose (irradiance × time) received by all samples in these experiments was 1.2 Ws/cm^2, calculated to be equal to an average bleaching dose received by the specimens in both the in vivo and in vitro FRAP experiments. The increased beam intensity due to the use of a higher magnification objective in the in vivo experiments was offset by placing neutral density filters into the beam.

Both enzymatic and actin-gelling activities of Rh-aldolase were reduced by the irradiation dose in these experiments: 56% of enzymatic activity (Fig. 5), and >50% of actin-gelling activity (Fig. 6) remained after irradiation. It is interesting to note that while actin-gelling activity was more sensitive to overlabeling, enzymatic activity was more sensitive to irradiation. Additionally, although no change was evident in the actin-gelling activity of the unlabeled control after irradiation, its enzymatic activity decreased almost as much as that of the labeled molecule upon irradiation. This is not unreasonable considering the substantial absorbance of the unlabeled control solution at the irradiation wavelength of 514 nm (0.006 vs. 0.033 for Rh-aldolase solution).

Rh-Aldolase Binds to Actin In Vitro

The actin-gelling activity demonstrated above is consistent with at least bivalent binding of aldolase to actin. If Rh-aldolase does indeed bind to actin, then we would expect a reduced diffusion coefficient, an immobile fraction, or both, when we measured the mobility of aldolase in the presence of actin. We confirmed this prediction by performing in vitro FRAP measurements of Rh-aldolase under conditions similar to those used for falling ball viscometry (Table II).

Rh-aldolase had an average mobility of $D_{37,aq} = 4.72 \times 10^{-7}$ cm^2/s, with no immobile fraction, and the presence of a 100-fold molar excess of FDP did not significantly affect these values. However, when we measured its diffusion coefficient in the presence of 1 mg/ml F-actin, we saw two distinct changes: $D_{37,aq}$ decreased to 1.04×10^{-7} cm^2/s, and there was a 36.3% immobile fraction. The observation of both an immobile fraction and a reduced D_{aq} suggests that several time constants of recovery are involved for Rh-aldolase–F-actin, and is consistent with multivalent binding of aldolase to actin. Successive FRAP measurements in the

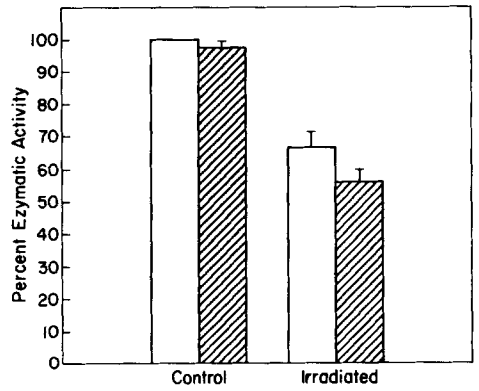

Figure 5. Effect of irradiation on enzymatic activity of aldolase and Rh-aldolase. 1.0 μM control aldolase (*open bars*) and Rh-aldolase (*hatched bars*) were irradiated with 120 Ws/cm^2 at 514 nm; 100% is defined as the activity of unlabeled control aldolase.

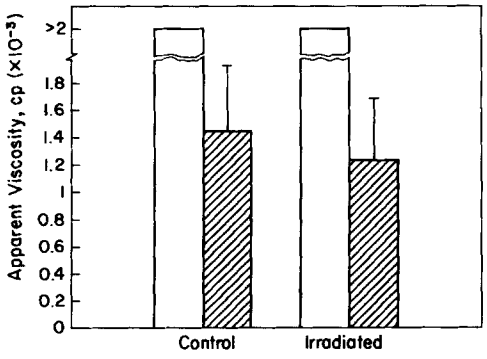

Figure 6. Effect of irradiation on actin-gelling activity of unlabeled control aldolase and Rh-aldolase. The low-shear viscosity of mixtures containing 1.5 μM aldolase (*open bars*) or Rh-aldolase (*hatched bars*) and 1.0 mg/ml F-actin was measured before and after irradiation as for Fig. 5. No difference was detected in the activities of irradiated and unirradiated control aldolase.

Table II. In Vitro FRAP Data

Sample	n*	$D_{20,aq} \times 10^7$‡	$D_{37,aq} \times 10^7$	Percent mobile
Rh-aldolase (1 μM)	26	3.08 ± 1.16§	4.72 ± 1.78	101.7 ± 6.9
Rh-aldolase + FDP (100 μM)	12	3.12 ± 1.23	4.78 ± 1.88	96.1 ± 9.6
Rh-aldolase + F-Actin (1 mg/ml)	20	0.68 ± 0.08	1.04 ± 0.12	63.7 ± 10.4
Rh-aldolase + FDP + F-Actin	26	2.72 ± 1.02	4.18 ± 1.57	98.6 ± 5.1
FD150 (1 μM)	10	3.15 ± 0.37	4.84 ± 0.57	106.2 ± 5.4
FD150 + Aldolase + F-Actin	14	2.84 ± 0.19	4.35 ± 0.29	102.8 ± 4.9

* Number of measurements used in calculating the mean.
‡ Aqueous diffusion coefficients (cm^2/s) were measured at 22–24°C and normalized to 20 ($D_{20,aq}$) and 37°C ($D_{37,aq}$) for comparison to in vivo data; see Materials and Methods for method.
§ Mean ± SD.

same spot (repeat FRAP) gave progressively greater recovery percentages (data not shown). The 4.5-fold decrease in diffusion coefficient, and the appearance of a significant immobile fraction were largely reversed when 100 μM FDP was included in the aldolase–actin mixture.

FD150 had no immobile fraction, and only a slight reduction of diffusion coefficient in the aldolase–F-actin gel. Even in the absence of actin-binding activity of FD150, diffusion barrier theory (53) predicts a 6–10% lower diffusion coefficient in the F-actin–aldolase gel, due to the obstructions of the gel network. Our data are consistent with this prediction.

The Cellular Distribution of Aldolase Is Relatively Uniform

Imaging cells coinjected with Rh-aldolase and FITC-dextran revealed that aldolase was distributed in a pattern similar to that of a dextran of a comparable size (Fig. 7). Both molecules were excluded from the nucleus and from vesicles, but distributed into the cell periphery equally well. Images of injected cells were remarkably uniform from 30 min to 24 h postinjection, demonstrating that Rh-aldolase integrated rapidly into a stable cellular pool of aldolase, and did not significantly affect cell viability. A notable exception to equal distribution of Rh-aldolase and FITC-dextran fluorescence

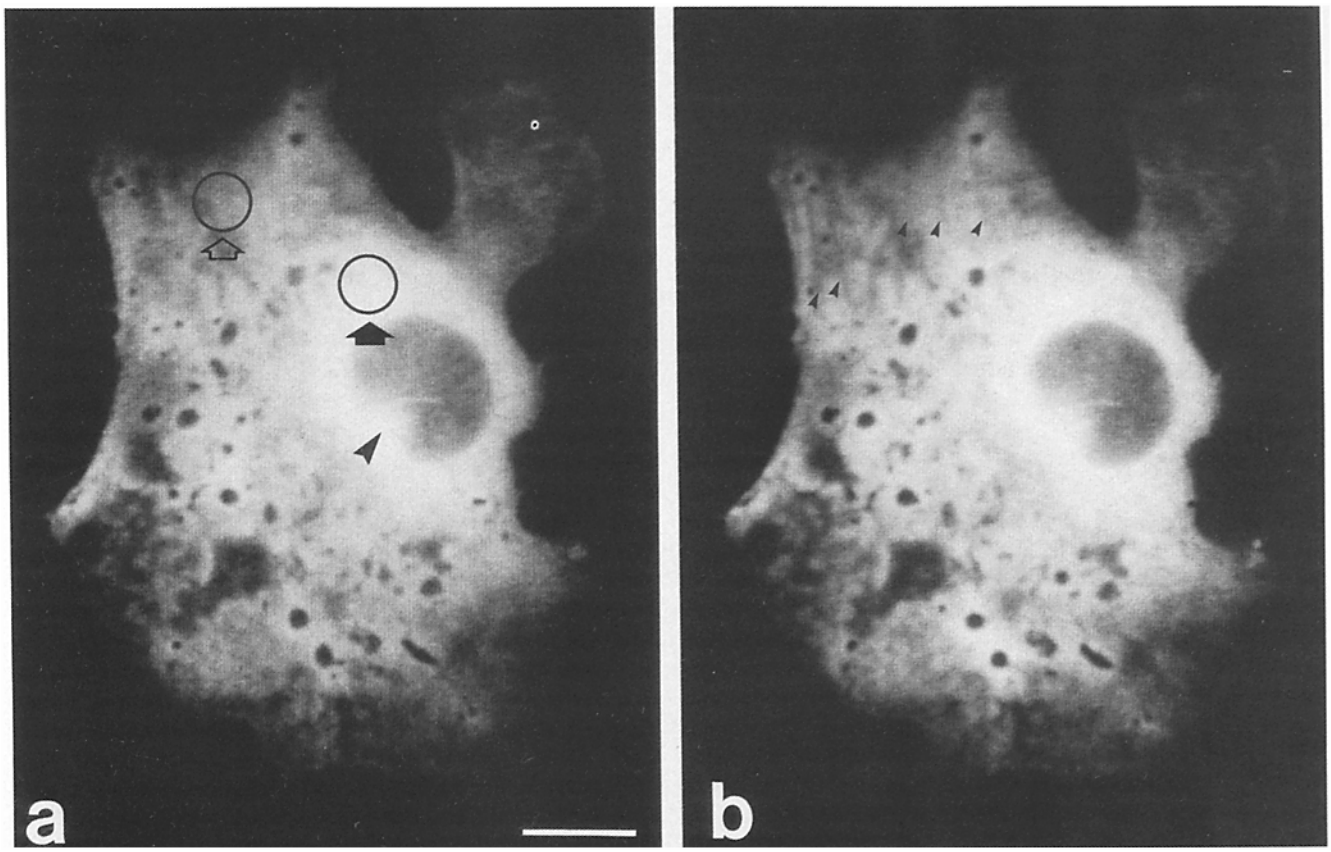

Figure 7. Fluorescence images of a cell coinjected with Rh-aldolase and FITC-dextran. Images of a 3T3 cell coinjected with Rh-aldolase (*a*) and FITC-dextran (*b*) are compared; typical perinuclear (*solid arrow*) and peripheral (*open arrow*) FRAP sites are shown. Large arrowhead in *a* indicates centrosome, small arrowheads in *b* mark stress fiber exclusion of dextran. Bar, 10 μm.

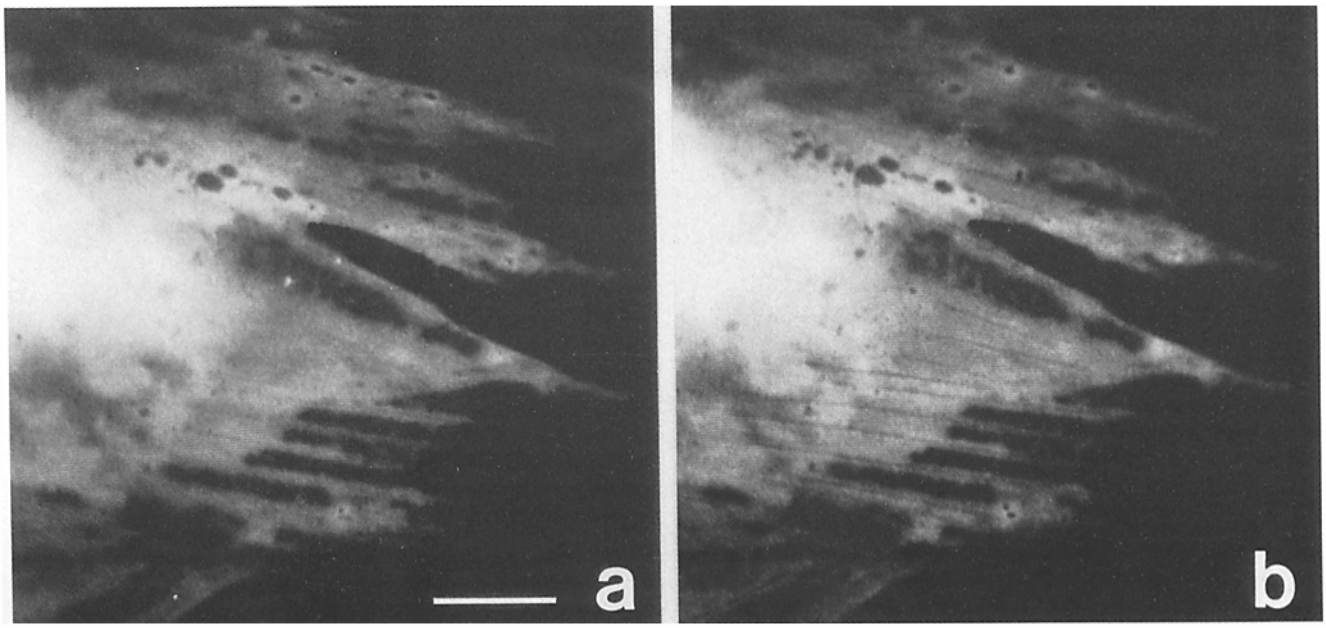

Figure 8. Fluorescence images of a coinjected cell. Rh-aldolase (*a*) and FITC-dextran (*b*) images of a stress fiber–rich region of a cell; note clear stress fiber exclusion in *b*. Bar, 10 μm.

was evident in the periphery of cells with well developed stress fibers. In the Rh-aldolase images, stress fibers could be detected by a slight negative staining effect (Figs. 7 *a* and 8 *a*; see reference 2). However, in the FITC-dextran images, much more dramatic exclusion of FITC-dextran from zones around stress fibers was evident at the same plane of focus (Figs. 7 *b* and 8 *b*).

To normalize the aldolase image in Fig. 8 for effects of pathlength and accessible volume on fluorescence intensity, we generated a ratio image in which Rh-aldolase fluorescence was divided by FITC-dextran fluorescence; bright areas in this image have a high concentration of aldolase relative to dextran (12, 70, 77). A relatively increased concentration of Rh-aldolase in zones around stress fibers is visualized as the bright, thin lines in Fig. 9. FITC-dextran is relatively excluded from these areas. Bright regions around cell periphery are probably due to movement of the cell between successive images. The relatively small differences in distribution we detected between Rh-aldolase and FITC-dextran are significant due to their location, and due to the spatial differences in aldolase mobility (see below).

Spatial Differences in Aldolase Mobility Exist In Vivo

We used FRAP measurements to determine the mobility of Rh-aldolase and FITC-dextran in living cells. It quickly became apparent that there were significant spatial differences in aldolase mobility within individual cells. Consequently, we performed FRAP measurements in two locations: perinuclear and peripheral regions as shown in Fig 7 *a*. Peripheral FRAP sites were areas with well-developed stress fibers (20–40% of beam area) visible by phase contrast. The data from these experiments are presented in Table III.

In the perinuclear region, aldolase had a D_{cyto} of 1.1×10^{-7} cm^2/s, a value 4.5-fold lower than its aqueous diffusion coefficient. This reduction may be explained simply by the higher viscosity of the aqueous phase of the cytoplasm, which has been reported to be between 3 and 6 centipoise (40, 42, 51, 55). However, the immobile fraction of 23% is not explained by cytoplasmic viscosity, and may reflect a bound fraction of aldolase in the perinuclear region. No immobile fraction was evident in the cell periphery, but the diffusion coefficient was 6.28×10^{-8} cm^2/s, about twofold lower than that of the perinuclear region.

Repeat FRAP in several perinuclear sites showed that a majority of the immobile fraction of Rh-aldolase was bleached by the initial measurement. The diffusion coefficient of the mobile fraction of Rh-aldolase in the second measurement was only slightly lower than in the original measurement at those spots. Since the repeat FRAP measurements followed the initial measurements by several minutes, these data establish that if the apparent immobile fraction we observed was, in fact, a very low mobility fraction, then its mobility must be at least several orders of magnitude lower than that of the higher mobility fraction (37).

We found no immobile fraction of FITC-dextran in either perinuclear or peripheral regions. The diffusion coefficients of FITC-dextran were intermediate between the two aldolase values and in good agreement with published in vivo values for similarly sized dextrans (44). The lack of difference in the perinuclear and peripheral mobilities of FITC-dextran rules out significant effects of cell geometry on measured values of D_{cyto}.

Discussion

We have identified an immobile fraction of Rh-aldolase in the perinuclear region of living 3T3 cells, and we also found spatial variation in its D_{cyto}. Coinjected FITC-dextran shows neither an immobile fraction nor spatial variations in mobility. These experiments are direct evidence that a fraction of aldolase partitions into the solid phase of living cytoplasm.

Previous studies demonstrated, using immunofluores-

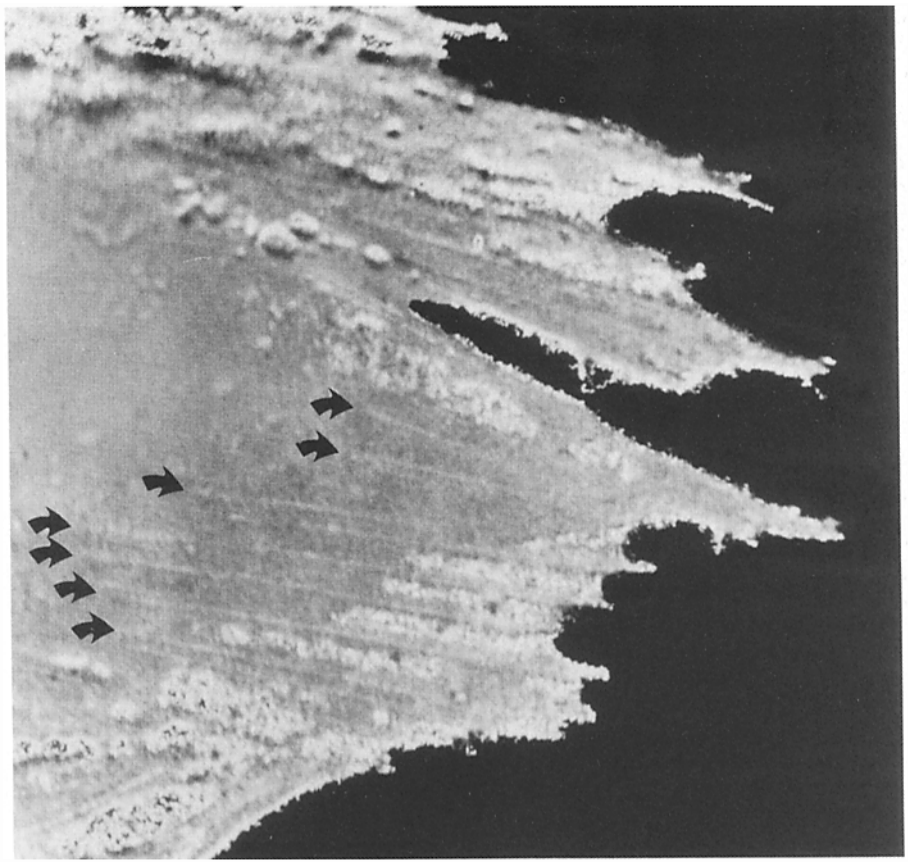

Figure 9. Ratio image. The Rh-aldolase image of Fig. 8 *a* divided by the FITC-dextran image of Fig. 8 *b*; arrows indicate high-ratio area around stress fibers. See text for discussion.

cence, that pyruvate kinase (22) and glyceraldehyde-3-phosphate dehydrogenase (21) have distributions very similar to actin in stress fibers, although this has not yet been demonstrated with aldolase. The uniform distribution of Rh-aldolase we observed in vivo initally seemed paradoxical, in light of data demonstrating that aldolase binds to F-actin (7, 15, 16), skeletal muscle homogenates (19), and fetal brain homogenates (17) with affinities greater than or equal to those of other glycolytic enzymes. However, the spatial differences we measured in the mobile fraction and diffusion coefficient of Rh-aldolase indicate that a sensitive equilibrium may regulate the actin-binding activity of aldolase in vivo. Therefore, localization of proteins such as aldolase to actin fibers based on immunofluorescence data could lead to a false impression about the true dynamics of the interactions.

Table III. In Vivo FRAP Data

	n*	$D_{37,cyto} \times 10^8$‡	Percent mobile
Rhodamine-aldolase			
Perinuclear	15	11.0 ± 3.31§	76.9 ± 6.7
Peripheral	19	5.73 ± 2.16	107.2 ± 5.6
Repeat perinuclear	5	9.40 ± 3.80	96.6 ± 3.7
FITC-dextran			
Perinuclear	12	6.86 ± 2.20	102.5 ± 8.5
Peripheral	13	6.28 ± 1.96	100.8 ± 8.6

* Number of measurements used in calculating the mean.
‡ Cytoplasmic diffusion coefficients (cm^2/s) were measured at 37°C.
§ Mean ± SD.

Evidence for a Microdomain of Aldolase Around Stress Fibers

We have considered two models to explain our in vivo data: hindered cytoplasmic diffusion and dynamic equilibrium. First, increasingly hindered diffusion, or higher microviscosity, in peripheral cytoplasm could account for the twofold lower peripheral D_{cyto} of Rh-aldolase (Table III). However, at least two lines of evidence argue against this model: (*a*) it does not by itself account for the perinuclear immobile fraction, and (*b*) the relative lack of spatial difference in the diffusion coefficient of our FITC-dextran control is inconsistent with this model.

The second model, which we favor, is based on an on/off rate for the aldolase–actin interaction in the cell periphery which is faster than we have resolved. This could be explained by a dynamic equilibrium between aldolase, actin, and FDP. Such an equilibrium could create a microdomain not only of aldolase, but of glycolytic activity around actin filaments and would be compatible with the dynamic equilibrium model proposed by Masters (48). The second model is also consistent with the fact that aldolase binds to the detergent resistant cytoskeleton in a variety of systems (32, 35, 36, 60). Our evidence for spatial differences in aldolase mobility suggests that local differences in cell metabolism could significantly affect the degree to which aldolase binds to actin. For example, glycolytic metabolism might be more important in the mitochondrion-poor cell periphery than in the perinuclear region. Energetically, the cell may not be able to afford an immobile fraction of aldolase in the periphery

if it is actively turning over substrate, and is thus inhibited from binding to actin. Presumably, there would be corresponding spatial heterogeneity in FDP concentrations, though this has not been demonstrated.

Even though the interactions between glycolytic enzymes, their substrates, and actin may be relatively weak, they must nonetheless be extremely important due to the very high local concentrations of these molecules around isotropically organized actin filaments and/or stress fibers. If indeed dynamic microdomains of glycolytic activity exist, we would expect these areas to relatively exclude inert molecules. Our data showing selective exclusion of FITC-dextran from regions around stress fibers are consistent with this prediction, as well as with a model in which glycolytic enzymes would exist in arrays around the actin cytoskeleton. The slight exclusion of Rh-aldolase from stress fibers (Fig. 8 *a*) suggests that it binds primarily to the surface, and does not integrate into the interior of fibers. Some glycolytic enzymes may not be directly associated with actin, but instead may be bound indirectly, in a "piggy-back" fashion on other glycolytic enzymes (22). It is important to point out that a solid state model such as this does not imply that a series of enzymes would be truly immobilized, or static. Rather, they would be confined to a microdomain in which the time-averaged probability of specific arrays and sequences occurring would be far higher than if the enzymes were freely soluble.

A truly immobilized enzyme fraction, such as the perinuclear aldolase fraction we have described, might represent a kinetically distinct subset. The phenomenon of ambiguity has been suggested for the association of hexokinase with the mitochondrial membrane (79). Other glycolytic enzymes may also be ambiguous; for example, binding of enzymes to actin may act essentially as an allosteric effector in vivo (50), since it has been demonstrated in vitro that actin-binding can modify both the K_m and V_{max} of aldolase by two orders of magnitude under appropriate conditions (74). Another result of the binding of glycolytic enzymes to actin would be competition between glycolytic enzymes and other actin-binding proteins (e.g., myosin) for binding sites on actin. A complex and sensitive regulatory system coupling cytoplasmic structure, motility, and glycolysis could result.

Evidence That the Perinuclear Immobile Fraction of Aldolase Represents a Specific Interaction

One possible important objection to direct comparison of cytoplasmic diffusion coefficients of molecules conjugated to different fluorochromes concerns differing interactions of various fluorochromes with intracellular components. As a control for this, all fluorochromes to be used must be bound to similar tracer particles, and their cytoplasmic diffusion coefficients measured. Changes in the mobile fraction are of particular concern, as they may represent selective partitioning of tracers labeled with hydrophobic fluorochromes into membrane compartments. This concern has been addressed for a range of particle sizes using both rhodamine- and fluorescein-labeled dextrans with the finding that no significant fluorochome based differences in D_{cyto} exist (43). This finding indicates that the mobilities of rhodamine- and fluorescein-labeled analogs may be accurately compared in vivo.

A second important concern is possible photooxidative cross-linking or breakage of filaments (or other cell components) caused by the irradiation used in FRAP and extended imaging experiments. There is recent evidence that bleaching irradiation doses used in FRAP experiments can create artifacts in populations of both labeled and unlabeled actin in vitro (63). Consequently, measurements of the effects of irradiation on analogue activity should be considered an essential part of experiments with biologically active fluorescent analogues. Our in vitro FRAP evidence that Rh-aldolase diffuses at the predicted rate in the presence of F-actin and excess FDP (Table II) demonstrates that the bleaching irradiation used neither cross-links nor disrupts actin filaments significantly. Additionally, the fraction of Rh-aldolase which absorbs a bleaching dose of irradiation in FRAP experiments (2–4%) retains much of its actin-binding and enzymatic activities. Since Rh-aldolase constitutes a small percentage of the cellular pool of aldolase (see below), the activity lost is unlikely to affect metabolism significantly.

How Much Aldolase Is in Cells?

As an initial estimate for cellular concentrations of aldolase, actin, and FDP, we have used the extensive literature on striated muscle glycolytic enzymes and intermediates, combined with data on nonmuscle cell volumes and protein concentrations. We will consider intracellular actin concentration as a reference point, since it has been shown to make up ~10% (wt/wt) of total protein of nonmuscle cells (57). Assuming an average mammalian cellular protein content of ~0.75 ng (76), and an average volume of $\sim 4 \times 10^{-12}$ liter (1), there would be $\sim 10^9$ actin molecules/cell (72). This results in a cellular actin concentration of ~19 mg/ml, consistent with a total cellular protein concentration of ~200 mg/ml (66, 67). If we assume that approximately half the total cellular volume is cytoplasmic, due to the volume fraction of mitochondria, vesicles, and endoplasmic reticulum, then the net actin concentration would be ~40 mg/ml, or 900 μM.

Srere (65) reported muscle tissue aldolase concentrations of 4.5×10^{-5} mol/kg, which equals ~7 mg/ml when averaged over total tissue weight. If we again assume that approximately half of the total cellular volume is cytoplasmic[4], the next aldolase concentration would be ~14 mg/ml, or 88 μM. This is $\sim 10^8$ molecules/cell, or 10-fold fewer aldolase tetramers than actin monomers. Since actin is not uniformly distributed in cells, however, the local actin/adolase ratio may vary considerably.

For in vivo FRAP experiments, we injected cells with $\sim 10^{-13}$ l (~10% of a cell volume) of a solution containing 2–4 mg/ml aldolase. Based on the calculations above, this would be an injection of analog equaling 2–4% of the total cellular pool of aldolase. This fraction is small enough that it is likely to rapidly incorporate into the cellular pool, and unlikely to affect normal metabolism significantly. A fraction much smaller than this would result in a weaker fluorescence signal with corresponding difficulties in detection.

The disparity between our detailed biochemical understanding of glycolysis and our lack of knowledge about the spatial organization of glycolysis in cytoplasm has been a dilemma for modern biology. Since glycolytic enzymes are such abundant cytoplasmic proteins, understanding the orga-

4. Nuclei in a variety of tissues have been shown to contain all the glycolytic enzymes (54); consequently, nuclear volume cannot be subtracted from total cell volume for the purpose of computing net cytoplasmic volume.

nization of glycolysis in living cells will significantly enhance our knowledge not only of glycolysis, but of the nature of cytoplasm. The approach we describe will be useful with other enzymes and could be a significant tool in characterizing metabolism in vivo.

Ray Griffith provided technical assistance throughout this project, and Robbin DeBiasio and Charlotte Bartosh maintained our cell culture facility. Fred Lanni, Albert Gough, Hou Li, and John Simon designed and constructed the FRAP instrument and continue to improve both the software and hardware. Gary Bright, Robbin DeBiasio, and Kate Luby-Phelps assisted patiently with microinjection and imaging. Finally, we thank Gary Bright, Lauren Ernst, Albert Gough, David Hackney, Alan Koretsky, Fred Lanni, Kate Luby-Phelps and Annemarie Weber for their many helpful discussions and critical comments on the manuscript.

This work has been supported by grant 2044 from the Council for Tobacco Research USA, Inc., and the National Institutes of Health Program Project Grant GM34639.

Received for publication 22 January 1988, and in revised form 17 May 1988.

References

1. Alberts, B., D. Bray, J. Lewis, M. Raff, K. Roberts, and J. D. Watson. 1983. Molecular Biology of the Cell. Garland Publishing, Inc., New York. 1146 pp.
2. Amato, P. A., and D. L. Taylor. 1986. Probing the mechanism of incorporation of fluorescently labeled actin into stress fibers. *J. Cell Biol.* 102:1074–1084.
3. Amato, P. A., E. R. Unanue, and D. L. Taylor. 1983. Distribution of actin in spreading macrophages: comparative study on living and fixed cells. *J. Cell Biol.* 96:750–761.
4. Anderson, C. W., P. R. Baum, and R. F. Gesteland. 1973. Processing of adenovirus 2-induced proteins. *J. Virol.* 12:241–252.
5. Arnold, H., and D. Pette. 1968. Binding of glycolytic enzymes to structure proteins of the muscle. *Eur. J. Biochem.* 6:163–171.
6. Arnold, H., and D. Pette. 1970. Binding of aldolase and triosephosphate dehydrogenase to F-actin and modification of catalytic properties of aldolase. *Eur. J. Biochem.* 15:360–366.
7. Arnold, H., R. Henning, and D. Pette. 1971. Quantitative comparison of the binding of various glycolytic enzymes to F-actin and the interaction of aldolase with G-actin. *Eur. J. Biochem.* 22:121–126.
8. Arnold, H., J. Nolte, and D. Pette. 1969. Quantitative and histochemical studies on the desorption and readsorption of aldolase in cross-striated muscle. *J. Histochem. Cytochem.* 17:314–320.
9. Axelrod, D., D. E. Koppel, J. Schlessinger, E. Elson, and W. W. Webb. 1976. Mobility measurement by analysis of fluorescence photobleaching recovery kinetics. *Biophys. J.* 16:1055–1069.
10. Deleted in proof.
11. Bolton, A. E., and W. M. Hunter. 1973. The labeling of proteins to high specific radioactivities by conjugation to a 125I-containing acylating agent. *Biochem. J.* 133:529–539.
12. Bright, G. R., G. W. Fisher, J. Rogowska, and D. L. Taylor. 1987. Fluorescence ratio imaging microscopy: temporal and spatial measurements of cytoplasmic pH. *J. Cell Biol.* 104:1019–1033.
13. Clarke, F. M., and C. J. Masters. 1973. Multi-enzyme aggregates: new evidence for an association of glycolytic components. *Biochim. Biophys. Acta.* 327:223–226.
14. Clarke, F. M., and C. J. Masters. 1974. On the association of glycolytic components in skeletal muscle extracts. *Biochim. Biophys. Acta.* 358:193–207.
15. Clarke, F. M., and C. J. Masters. 1975. On the association of glycolytic enzymes with structural proteins of skeletal muscle. *Biochim. Biophys. Acta.* 318:37–46.
16. Clarke, F. M., and D. J. Morton. 1976. Aldolase binding to actin-containing filaments: formation of paracrystals. *Biochem. J.* 159:797–798.
17. Clarke, F. M., and D. J. Morton. 1982. Glycolytic enzyme binding in fetal brain—the role of actin. *Biochem. Biophys. Res. Commun.* 109:388–393.
18. Clarke, F. M., D. J. Morton, P. Stephan, and J. Wiedemann. 1985. The functional duality of glycolytic enzymes: potential integrators of cytoplasmic structure and function. *In* Cell Motility: Mechanism and Regulation (10th Yamada Conference). H. Ishikawa, S. Hatano, and H. Sato, editors. Tokyo University Press, Tokyo. 235–250.
19. Clarke, F. M., F. D. Shaw, and D. J. Morton. 1980. Effect of electrical stimulation *post mortem* of bovine muscle on the binding of glycolytic enzymes: functional and structural implications. *Biochem. J.* 186:105–109.
20. Clarke, F. M., P. Stephan, G. Huxham, D. Hamilton, and D. J. Morton. 1984. Metabolic dependence of glycolytic enzyme binding in rat and sheep heart. *Eur. J. Biochem.* 138:643–649.
21. Clarke, F. M., P. Stephan, D. Morton, and J. Wiedemann. 1983. The role of actin and associated structural proteins in the organisation of glycolytic enzymes. *In* Actin: Structure and Function in Muscle and Non-muscle Cells. C. dos Remedios and J. Barden, editors. Academic Press, Inc., New York. 249–257.
22. Clarke, F. M., P. Stephan, D. J. Morton, and J. Wiedemann. 1985. Glycolytic enzyme organization via the cytoskeleton and its role in metabolic regulation. In Regulation of Carbohydrate Metabolism. Vol. 2. R. Beitner, editor. CRC Press, Inc., Boca Raton, Florida. 1–31.
23. Clegg, J. S. 1984. Properties and metabolism of the aqueous cytoplasm and its boundaries. *Am. J. Physiol.* 246:R133–R151.
24. Craig, S. W., and T. D. Pollard. 1982. Actin-binding proteins. *Trends in Biochem. Sci.* 7:88–92.
25. DeBiasio, R., G. R. Bright, L. A. Ernst, A. S. Waggoner, and D. L. Taylor. 1987. Five-parameter fluorescence imaging: wound healing of living Swiss 3T3 cells. *J. Cell Biol.* 105:1613–1622.
26. de Duve, C. 1972. Is there a glycolytic particle? *In* Structure and Function of Oxidation-Reduction Enzymes. A. Akeson and A. Ehrenberg, editors. Pergamon Press, Inc., Oxford. 715–728.
27. Dolken, G., E. Leisner, and D. Pette. 1975. Immunofluorescent localization of glycogenolytic and glycolytic enzyme proteins and of malate dehydrogenase isozymes in cross-striated skeletal muscle and heart of the rabbit. *Histochem. J.* 43:113–121.
28. Ernster, L., and G. Schatz. 1981. Mitochondria: a historical review. *J. Cell Biol.* 91:227s–255s.
29. Fowler, V. M., and H. B. Pollard. 1982. In vitro reconstitution of chromaffin granule-cytoskeleton interactions: ionic factors influencing the association of F-actin with purified chromaffin granule membranes. *J. Cell. Biochem.* 18:295–311.
30. Fowler, V. M., and D. L. Taylor. 1980. Spectrin plus band 4.1 cross-link actin: regulation by micromolar calcium. *J. Cell Biol.* 85:361–376.
31. Fulton, A. B. 1982. How crowded is the cytoplasm? *Cell.* 30:345–347.
32. Gilbert, M., and A. B. Fulton. 1985. The specificity and stability of the Triton-extracted cytoskeletal framework of gerbil fibroma cells. *J. Cell Sci.* 73:335–345.
33. Heidner, E. G., B. H. Weber, and D. Eisenberg. 1971. Subunit structure of aldolase. *Science (Wash. DC).* 171:677–680.
34. Hubscher, G., R. J. Mayer, and H. J. M. Hansen. 1971. Glycolytic enzymes as a multi-enzyme system. *Bioenergetics.* 2:115–118.
35. Humphreys, L., and C. Masters. 1986. On the differential release of glycolytic enzymes from cellular structure. *Biochem. Int.* 13:71–77.
36. Knull, H. R. 1985. Extraction of glycolytic enzymes: myo-inositol as a marker of membrane porosity. *J. Neurochem.* 45:1433–1440.
37. Kreis, T. E., B. Geiger, and J. Schlessinger. 1982. Mobility of microinjected rhodamine actin within living chicken gizzard cells determined by fluorescence photobleaching recovery. *Cell.* 29:835–845.
38. Laemmli, U. K. 1970. Cleavage of structural proteins during the assembly of the head of bacteriophage T4. *Nature (Lond.).* 227:680–685.
39. Lai, C. Y., N. Nakai, and D. Chang. 1974. Amino acid sequence of rabbit muscle aldolase and the structure of the active center. *Science (Wash. DC).* 183:1204–1206.
40. Lepock, J. R., K. Cheng, S. D. Campbell, and J. Kruv. 1983. Rotational diffusion of tempone in the cytoplasm of Chinese hamster lung cells. *Biophys. J.* 44:405–412.
41. Lowry, O. H., N. J. Rosebrough, A. L. Farr, and R. J. Randall. 1951. Protein measurement with the Folin phenol reagent. *J. Biol. Chem.* 193: 265–275.
42. Luby-Phelps, K., P. E. Castle, D. L. Taylor, and F. Lanni. 1987. Hindered diffusion of inert tracer particles in the cytoplasm of mouse 3T3 cells. *Proc. Natl. Acad. Sci. USA.* 84:4910–4913.
43. Luby-Phelps, K., F. Lanni, and D. L. Taylor. 1985. Behavior of a fluorescent analogue of calmodulin in living 3T3 cells. *J. Cell Biol.* 101: 1245–1256.
44. Luby-Phelps, K., D. L. Taylor, and F. Lanni. 1986. Probing the structure of cytoplasm. *J. Cell Biol.* 102:2015–2022.
45. MacLean-Fletcher, S. D., and T. D. Pollard. 1980. Viscometric analysis of the gelation of *Acanthamoeba* extracts and purification of two gelation factors. *J. Cell Biol.* 85:414–428.
46. Masters, C. J. 1977. Metabolic control and the microenvironment. *Curr. Top. Cell. Regul.* 12:75–105.
47. Masters, C. J. 1981. Interactions between soluble enzymes and subcellular structure. *CRC Crit. Rev. Biochem.* 11:105–143.
48. Masters, C. J. 1984. Interactions between glycolytic enzymes and components of the cytomatrix. *J. Cell Biol.* 99(Suppl):222s–225s.
49. Masters, C. J., and D. J. Winzor. 1971. The molecular size of enzymatically active aldolase A. *Biochem. J.* 121:735–736.
50. Masters, C. J., R. J. Sheedy, D. J. Winzor, and L. W. Nichol. 1969. Reversible adsorption of enzymes as a possible allosteric control mechanism. *Biochem. J.* 112:806–808.
51. Mastro, A. M., M. A. Babich, W. D. Taylor, and A. D. Keith. 1984. Diffusion of a small molecule in the cytoplasm of mammalian cells. *Proc. Natl. Acad. Sci. USA.* 81:3414–3418.
52. Morton, D. J., F. M. Clarke, and C. J. Masters. 1977. An electron microscope study of the interaction between fructose diphosphate aldolase and actin-containing filaments. *J. Cell Biol.* 74:1016–1023.
53. Ogston, A. G., B. N. Preson, and J. D. Wells. 1973. On the transport of compact particles through solutions of chain-polymers. *Proc. R. Soc.*

Lond. A. 333:297–316.
54. Ottaway, J. H., and J. Mowbray. 1977. The role of compartmentation in the control of glycolysis. *Curr. Top. Cell. Regul.* 12:107–208.
55. Paine, P. L., and S. B. Horowitz. 1980. The movement of material between nucleus and cytoplasm. *In* Cell Biology: A Comprehensive Treatise. L. Goldstein and D. M. Prescott, editors. Academic Press, Inc., New York. 4:299–338.
56. Penhoet, E. E., and W. J. Rutter. 1975. Detection and isolation of mammalian fructose-diphosphate aldolases. *Methods Enzymol.* 42:240–249.
57. Pollard, T. D. 1981. Cytoplasmic contractile proteins. *J. Cell Biol.* 91 (Suppl.):156s–165s.
58. Racker, E. 1947. Spectrophotometric measurement of hexokinase and phosphohexokinase activity. *J. Biol. Chem.* 167:843–854.
59. Schacterle, G. R., and R. L. Pollack. 1973. A simplified method for the quantitative assay of small amounts of protein in biological material. *Anal. Biochem.* 51:654–655.
60. Schliwa, M., U. Euteneur, and K. R. Porter. 1987. Release of enzymes of intermediary metabolism from permeabilized cells: further evidence in support of a structural organization of the cytoplasmic matrix. *Eur. J. Cell Biol.* 44:214–218.
61. Sigel, P., and D. Pette. 1969. Intracellular localization of glycogenolytic and glycolytic enzymes in white and red rabbit skeletal muscle: a gel film method for coupled enzyme reactions in histochemistry. *J. Histochem. Cytochem.* 17:225–237.
62. Simon, J. R., and D. L. Taylor. 1986. Preparation of a fluorescent analog: acetamidofluoresceinyl-labeled *Dictyostelium discoideum* alpha-actinin. *Methods Enzymol.* 134:487–507.
63. Simon, J. R., A. Gough, E. Urbanik, F. Wang, B. R. Ware, and D. L. Taylor. 1988. Analysis of rhodamine and fluorescein-labeled F-actin diffusion in vitro by fluorescence photobleaching recovery. *Biophy. J.* In press.
64. Spudich, J. A., and S. Watt. 1971. The regulation of rabbit skeletal muscle contraction. *J. Biol. Chem.* 246:4866–4871.
65. Srere, P. A. 1967. Enzyme concentrations in tissues. *Science (Wash. DC)* 158:936–937.
66. Srivastava, D. K., and S. A. Bernhard. 1986. Enzyme-enzyme interactions and the regulation of metabolic reaction pathways. *Curr. Top. Cell. Regul.* 28:1–68.
67. Srivastava, D. K., and S. A. Bernhard. 1986. Metabolite transfer via enzyme-enzyme complexes. *Science (Wash. DC).* 234:1081–1086.
68. Standart, N. M., S. J. Bray, E. L. George, T. Hunt, and J. V. Ruderman. 1985. The small subunit of ribonucleotide reductase is encoded by one of the most abundant translationally regulated maternal RNAs in clam and sea urchin eggs. *J. Cell Biol.* 100:1968–1976.
69. Stewart, M., D. J. Morton, and F. M. Clarke. 1980. Interaction of aldolase with actin-containing filaments: structural studies. *Biochem. J.* 186: 99–104.
70. Tanasugarn, L., P. McNeil, G. Reynolds, and D. L. Taylor. 1984. Microspectrofluorometry by digital image processing: measurement of cytoplasmic pH. *J. Cell Biol.* 98:717–724.
71. Taylor, D. L., P. A. Amato, K. Luby-Phelps, and P. L. McNeil. 1984. Fluorescent analog cytochemistry. *Trends Biochem. Sci.* 9:88–91.
72. Taylor, D. L., P. A. Amato, P. L. McNeil, K. Luby-Phelps, and L. Tanasugarn. 1986. Spatial and temporal dynamics of specific molecules and ions in living cells. *In* Applications of Fluorescence in the Biomedical Sciences. D. L. Taylor, A. S. Waggoner, R. F. Murphy, and F. Lanni, editors. Alan R. Liss, Inc., New York. 347–376.
73. van Zoelen, E. J. J., L. G. J. Tertoolen, and S. W. de Laat. 1983. Simple computer method for evaluation of lateral diffusion coefficients from fluorescence photobleaching recovery kinetics. *Biophys. J.* 42:103–108.
74. Walsh, T. P., F. M. Clarke, and C. J. Masters. 1977. Modification of the kinetic parameters of aldolase on binding to the actin-containing filaments of skeletal muscle. *Biochem. J.* 165:165–167.
75. Walsh, T. P., D. J. Winzor, F. M. Clarke, C. J. Masters, and D. J. Morton. 1980. Binding of aldolase to actin-containing filaments: evidence of interaction with the regulatory proteins of skeletal muscle. *Biochem. J.* 186:89–98.
76. Wang, K., J. R. Feramisco, and J. F. Ash. 1982. Fluorescent localization of contractile proteins in tissue culture cells. *Methods Enzymol.* 85: 514–562.
77. Wang, Y. L., J. M. Heiple, and D. L. Taylor. 1982. Fluorescent analog cytochemistry of contractile proteins. *Methods Cell Biol.* 25(B):1–11.
78. Weast, R. C. 1974. CRC Handbook of Chemistry and Physics, 55th ed. CRC Press, Inc., Boca Raton, Florida. F-49.
79. Wilson, J. E. 1978. Ambiquitous enzymes: variation in intracellular distribution as a regulatory mechanism. *Trends in Biochem. Sci.* 3:124–125.
80. Wong, P., and E. T. Harper. 1982. Selective arylation of cysteine-237 of rabbit muscle aldolase with 4-chloro-7-nitrobenzofurazan. *Biochim. Biophys. Acta.* 700:33–41.
81. Yguerabide, J., J. A. Schmidt, and E. E. Yguerabide. 1982. Lateral mobility in membranes as detected by fluorescence recovery after photobleaching. *Biophys. J.* 39:69–75.